Synthetic and Systems Biotechnology 9 (2024) 269–276

Contents lists available at ScienceDirect

Synthetic and Systems Biotechnology

journal homepage: www.keaipublishing.com/en/journals/synthetic-and-systems-biotechnology

Original Research Article

Construction of an alternative NADPH regeneration pathway improves ethanol production in *Saccharomyces cerevisiae* with xylose metabolic pathway

Yali Qiu [a], Wei Liu [a], Meiling Wu [b], Haodong Bao [a], Xinhua Sun [a], Qin Dou [a], Hongying Jia [a], Weifeng Liu [a], Yu Shen [a,*]

[a] State Key Laboratory of Microbial Technology, Institute of Microbial Technology, Shandong University, Qingdao, 266237, China
[b] Advanced Medical Research Institute, Shandong University, Jinan, 250012, China

ARTICLE INFO

Keywords:
Saccharomyces cerevisiae
Xylose
Ethanol
NADPH
Glyceraldehyde-3-phosphate dehydrogenase

ABSTRACT

Full conversion of glucose and xylose from lignocellulosic hydrolysates is required for obtaining a high ethanol yield. However, glucose and xylose share flux in the pentose phosphate pathway (PPP) and glycolysis pathway (EMP), with glucose having a competitive advantage in the shared metabolic pathways. In this work, we knocked down *ZWF1* to preclude glucose from entering the PPP. This reduced the [NADPH] level and disturbed growth on both glucose or xylose, confirming that the oxidative PPP, which begins with Zwf1p and ultimately leads to CO_2 production, is the primary source of NADPH in both glucose and xylose. Upon glucose depletion, gluconeogenesis is necessary to generate glucose-6-phosphate, the substrate of Zwf1p. We re-established the NADPH regeneration pathway by replacing the endogenous NAD^+-dependent glyceraldehyde-3-phosphate dehydrogenase (GAPDH) gene *TDH3* with heterogenous $NADP^+$-GAPDH genes *GDH*, *gapB*, and *GDP1*. Among the resulting strains, the strain BZP1 (*zwf1Δ*, *tdh3*::*GDP1*) exhibited a similar xylose consumption rate before glucose depletion, but a 1.6-fold increased xylose consumption rate following glucose depletion compared to the original strain BSGX001, and the ethanol yield for total consumed sugars of BZP1 was 13.5% higher than BSGX001. This suggested that using the EMP instead of PPP to generate NADPH reduces the wasteful metabolic cycle and excess CO_2 release from oxidative PPP. Furthermore, we used a copper-repressing promoter to modulate the expression of *ZWF1* and optimize the timing of turning off the *ZWF1*, therefore, to determine the competitive equilibrium between glucose-xylose co-metabolism. This strategy allowed fast growth in the early stage of fermentation and low waste in the following stages of fermentation.

1. Background

Bioethanol has an increasingly critical role in reducing the greenhouse effect and enabling energy transitions, especially 2nd generation bioethanol produced from lignocellulose, which is a renewable energy source [1,2]. Xylose is the second most abundant sugar found in lignocellulosic hydrolysate after glucose [3–5]. Therefore, the full co-utilization of glucose and xylose represents a cost-effective approach for converting biomass feedstock into bioethanol [6]. *Saccharomyces cerevisiae* is an optimal cell factory due to its robust metabolic capacity and high tolerance to inhibitors [7–9]. However, it lacks the initial xylose metabolic pathway, and glucose use inhibits xylose utilization [10,11].

To generate the xylose metabolic pathway in *S. cerevisiae* strains, heterologous xylose isomerase (XI) or xylose reductase (XR) alongside xylitol dehydrogenase (XDH) was introduced into the strains to transform xylose to xylulose [12–15]. The XI pathway, involving only one isomerization step, is straightforward (Fig. 1). However, cofactor engineering, including altering the coenzyme preference, is necessary to resolve cofactor imbalance in the strain metabolizing xylose via the XR-XDH pathway, because XR prefers NADPH rather than NADH, while XDH only utilizes NAD^+ [15,16]. Efficient xylose-utilizing yeasts have

Peer review under responsibility of KeAi Communications Co., Ltd.
* Corresponding author: State Key Laboratory of Microbial Technology, Institute of Microbial Technology, Shandong University, Jimo Binhai Road 72, Qingdao, 266237, China.
E-mail address: shenyu@sdu.edu.cn (Y. Shen).

https://doi.org/10.1016/j.synbio.2024.02.004
Received 19 December 2023; Received in revised form 5 February 2024; Accepted 19 February 2024
Available online 28 February 2024

been obtained through further metabolic engineering, predominantly relying on overexpressing xylulokinase genes and non-oxidative pentose phosphate pathway (PPP) genes to elevate the downstream flux [17]. Additionally, deletion of the aldose reductase gene *GRE3* avoids the accumulation of xylitol [15], and adapting evolution in the medium using xylose as the lone or primary carbon source to reform the cellular regulatory system, thus improving xylose metabolic efficiency [18]. Nevertheless, the xylose metabolic capacity of these strains remains much lower than glucose [19,20], especially when exposed to glucose-xylose co-fermentation.

Xylose utilization is severely reduced by glucose both in the glucose stage and after glucose depletion [19,20]. Based on the common metabolic pathways, xylose is phosphorylated to xylulose, where it enters the PPP, and then enters the EMP as the intermediate metabolite glyceraldehyde-3-phosphate (G3P) and fructose-6-phosphate (F6P). While most glucose directly enters EMP, 10%–15% of glucose enters the PPP first (Fig. 1) [21]. This means glucose competes with xylose for flux throughout both the PPP and EMP. It is theoretically feasible to improve glucose and xylose co-fermentation by limiting the metabolic flux competition of glucose relative to xylose [22]. One successful approach is that Miskovic L et al. reduced the glucose metabolism rate by deleting the hexokinase gene *HXK2* [23], which reduced the rate of glucose phosphorylation, and improved glucose-xylose co-utilization. Similarly, blocking the oxidative PPP is another approach, leaving the PPP flux entirely to xylose.

However, the oxidative PPP is the primary source of NADPH, a key reducing agent required for general biosynthesis [24]. There are two reactions in the oxidative PPP that generate NADPH (Fig. 1). The first is the conversion of glucose-6-phosphate (G6P) to 6-phosphogluconolactone (6PGL) catalyzed by glucose-6-phosphate dehydrogenase, representing the rate-limiting step of PPP. Second is the conversion of 6-phosphogluconate (6 PG) to ribulose-5-phosphate, which is catalyzed by 6-phosphogluconate dehydrogenase, causing the release of a molecule of CO_2. Theoretically, blocking the oxidative PPP may limit the CO_2 emission, which could elevate the ethanol yield. However, constructing an efficient NADPH regeneration pathway may be a prerequisite for shutting down the PPP, as securing an adequate supply of NADPH is vital for the synthetic metabolism of the cell.

To improve xylose utilization and elevate ethanol yield, the *ZWF1* gene, which encodes glucose 6-phosphate dehydrogenase (G6PDH), was deleted from a xylose-utilizing recombinant *S. cerevisiae* strain BSGX001 [19]. This significantly decreased cell growth. To secure an adequate supply of NADPH, three heterologous $NADP^+$-dependent glyceraldehyde-3-phosphate dehydrogenase genes [25–27] were respectively expressed in the *zwf1Δ* strain in the position of the *TDH3* gene, which encodes a NAD^+-dependent glyceraldehyde-3-phosphate dehydrogenase. Among them, the expression of *GDP1* best compensated for the negative effects of *ZWF1* deletion with respect to cell growth and improved xylose utilization. Then the *CTR1* promoter, which can be inhibited by Cu^{2+} [28], was used to modulate the expression of *ZWF1* in the *GDP1* expressing strain. $CuSO_4$ was added to the fermentation broth at 8 and 12 h, respectively, to assess whether this strategy leads to faster cell growth in the early stage of fermentation and improved xylose utilization in subsequent stages, compared to the strategy of deleting *ZWF1*.

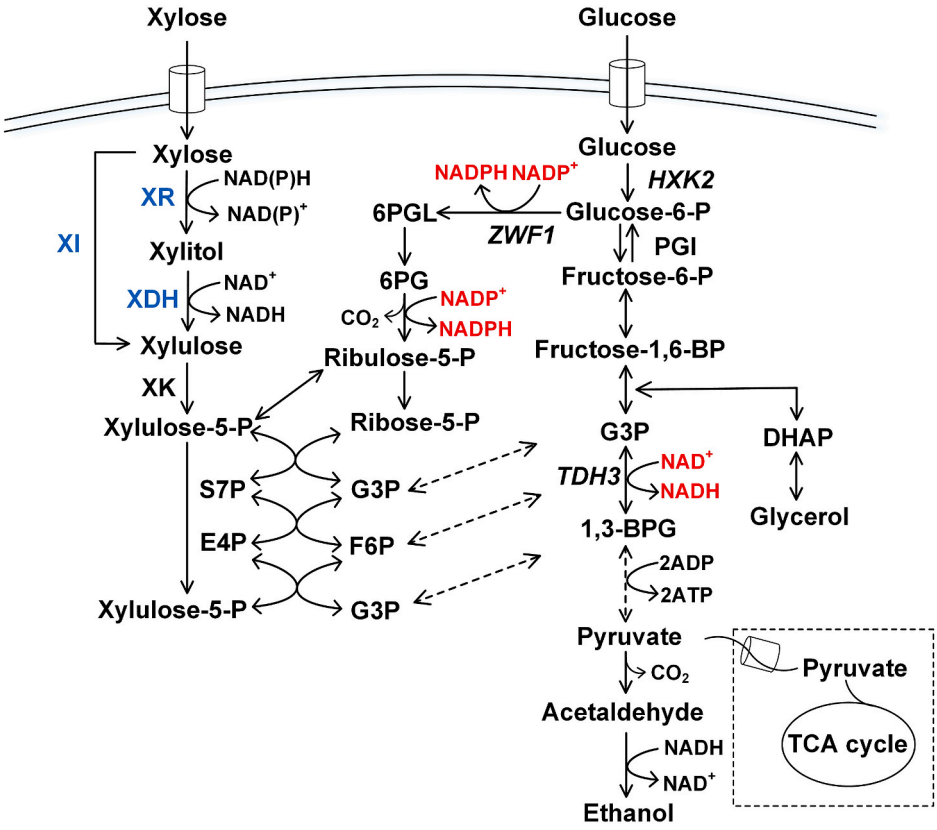

Fig. 1. The pathway of glucose and xylose co-metabolism in *S. cerevisiae*. 6PGL, 6-phosphogluconolactone; 6 PG, 6-phosphogluconate; G3P, glyceraldehyde-3-phosphate; F6P, fructose-6-phosphate; S7P, sedoheptulose-7-phosphate; E4P, erythrose-4-phosphate; 1,3-BPG, 1,3-diphosphoglycerate; DHAP, dihydroxyacetone phosphate; XI, xylose isomerase; XR, xylose reductase; XDH, xylitol dehydrogenase; XK, xylulokinase; *HXK2*, encoding hexokinase; PGI, phosphoglucose isomerase; *ZWF1*, encoding glucose-6-phosphate dehydrogenase; *TDH3*, encoding glyceraldehyde-3-phosphate dehydrogenase.

2. Methods

2.1. Strain construction

All *S. cerevisiae* strains used in this study are listed in Table 1. The BSGX001, a xylose utilizing recombinant strain with XI pathway [19], was employed as the parental strain. Other *S. cerevisiae* strains were successively derived from BSGX001. All expression and deletion procedures were controlled by manipulating genomic DNA using homologous recombination technology. All expression and deletion cassettes of transformants were confirmed via sequencing to obtain the target strain.

To delete *ZWF1* (NC_001146.8), the *natMX6* cassette was amplified out of the Cas9-NAT plasmid [29]. Two homologous arms, $ZWF1_{up}$ (−208 to 5 bp) and $ZWF1_{down}$ (1524–1776 bp), were amplified from the BSGX001 genomic DNA and fused with the *natMX6* cassette using overlap extension PCR. The resulting fragment $ZWF1_{up}$-*natMX6*-$ZWF1_{down}$ was transformed into BSGX001, and the correct transformant was named BZ. To replace *TDH3* (CP046087.1), which encodes glyceraldehyde-3-phosphate dehydrogenase (GAPDH), in the strain BZ with other GAPDHs, a *KanMX4* cassette was amplified from the pUG 6 plasmid [30]. The codon-optimized genes for GAPDH from *Spinacia oleracea* (*GDH*, NW_018932882.1) and *Kluyveromyces lactis* (*GDP1*, NC_006042.1) were artificially synthesized, while the *gapB* gene (NC_000964.3) was cloned from the genomic DNA of *Bacillus subtilis*. Two homologous arms, $TDH3_{up}$ (−188 to −1 bp) and $TDH3_{down}$ (999–1198 bp), were amplified from the BSGX001 genomic DNA. These were subsequently fused with the *KanMX4* cassette and the various GAPDH genes using overlap extension PCR. The fragments $TDH3_{up}$-*GDH-KanMX4*-$TDH3_{down}$, $TDH3_{up}$-*gapB-KanMX4*-$TDH3_{down}$, and $TDH3_{up}$-*GDP1-KanMX4*-$TDH3_{down}$ were individually transformed into the BZ strain. The correct transformants were named BZH, BZB, and BZP1, respectively.

The fragment $TDH3_{up}$-*GDP1-KanMX4*-$TDH3_{down}$ was also transformed into BSGX001 to obtain the strain BP1. The *CTR1* promoter, $ZWF1_{up}$ (−736 to −526 bp), and $ZWF1_{down}$ (0–214 bp) were amplified out of the BSGX001 genomic DNA, and then fused with the *natMX6* cassette through overlap extension PCR. The resulting fragment, $ZWF1_{up}$-*natMX6*-P_{CTR1}-$ZWF1_{down}$, was transformed into the strain BP1 to replace the original promoter of *ZWF1* with the *CTR1* promoter. The transformant carrying the genotype of *tdh3*::*GDP1-loxP-KanMX4-loxP*; P_{ZWF1}-*ZWF1*::P_{CTR1}-*ZWF1-nat* was named BP1R1.

2.2. Media and culture conditions

BSGX001 was cultured at 30 °C in synthetic complete dropout uracil (SC-Ura) medium [1.7 g L^{-1} yeast nitrogen base, 5 g L^{-1} ammonium sulfate, and 0.77 g L^{-1} CSM-Ura (Sunrise Science Products, USA)] supplemented with 20 g L^{-1} glucose as the carbon source. The derived strains were also cultured in SC-Ura supplemented with 20 g L^{-1} glucose, but G418 (Genview, China) (200 mg L^{-1} in liquid medium and 600 mg L^{-1} in solid medium) and nourseothricin (Gold Biotechnology, USA) (100 mg L^{-1} in liquid medium and 200 mg L^{-1} in solid medium) were supplemented as necessary. The fermentation medium YNB (pH 5.5) was composed of 1.7 g L^{-1} yeast nitrogen base and 5 g L^{-1} ammonium sulfate, 20 g L^{-1} glucose, and 20 g L^{-1} xylose were used as the carbon source. To turn off the *CTR1* promoter, 300 μM $CuSO_4$ was included in the fermentation broth at the designated time.

Table 1
S. cerevisiae strains used in this study.

Name	Description	Source
BSGX001	CEN.PK 113-5D derivative; XK, *gre3*::PPP, *cox4Δ*, AE[a], pJX7	[19]
BZ	BSGX001 derivative; *zwf1*:: *natMX6*	This study
BZH	BZ derivative; *tdh3*::*GDH-loxP-KanMX4-loxP*	This study
BZB	BZ derivative; *tdh3*::*gapB-loxP-KanMX4-loxP*	This study
BZP1	BZ derivative; *tdh3*::*GDP1-loxP-KanMX4-loxP*	This study
BP1	BSGX001 derivative; *tdh3*::*GDP1-loxP-KanMX4-loxP*	This study
BP1R1	BSGX001 derivative; *tdh3*::*GDP1-loxP-KanMX4-loxP*; P_{ZWF1}-*ZWF1*::P_{CTR1}-*ZWF1-nat*	This study

2.3. NADPH/$NADP^+$ assay

NADPH and $NADP^+$ were isolated from yeast cells and examined using a Coenzyme II NADP(H) Content Assay Kit (Solarbio, BC1105, Beijing, China). The $A_{570\ nm}$ of the reaction solution was determined using a Synergy™ HT MultiDetection Microplate Reader (Bio-Tek Instruments Inc., Vermont, USA). Protein quantification was conducted using the Enhanced BCA Protein Assay Kit (Beyotime, P0010, Shanghai, China) according to the manufacturer's directions. The yeast cells were grown in a YNB medium supplemented with 20 g L^{-1} glucose and 20 g L^{-1} xylose as carbon sources, and samples were taken at 16 h and 36 h.

2.4. Batch fermentation

A single colony was incubated in SC-Ura medium containing 20 g L^{-1} glucose, and cultured overnight. It was transferred to a 100-mL shaken flask containing 20 mL of fresh medium, with an initial OD_{600} of approximately 1.0. After 12 h of incubation at 30 °C and 200 rpm shaking, the cells were harvested and rinsed once with fermentation medium, and then inoculated into a 200-mL shaken flask containing 40 mL of fermentation medium, at an initial OD_{600} of approximately 0.5. A rubber stopper plug with a syringe needle generated the oxygen-limited condition. The fermentation was conducted at 30 °C and shaking at 200 rpm for 72 h. $CuSO_4$ was added to the fermentation broth as required.

2.5. Quantitative analysis

Cell growth was monitored by measuring the density (OD_{600}) of the culture using a UV–visible spectrophotometer (Eppendorf BioPhotometer D30, Germany). The concentrations of glucose, xylose, glycerol, acetate, and ethanol were characterized using HPLC (Shimadzu, Japan) alongside an Aminex HPX-87H ion exchange column (300 × 7.8 mm) (BioRad, Hercules, USA) at 45 °C, and a refractive index detector RID-10A (Shimadzu, Japan). The mobile phase consisted of 5 mM H_2SO_4 with a flow rate of 0.6 mL min^{-1} [31]. The maximum specific growth rates are the linear regression coefficients of the ln OD_{600} versus time throughout the exponential growth phase. The specific consumption/production rates of glucose, xylose, glycerol, acetate, and ethanol were determined as previously described [32].

2.6. Quantitative real-time PCR (qRT-PCR)

Quantitative real-time PCR was utilized to detect the transcriptional level of *ZWF1*. Total RNA was extracted using Trizol reagent. cDNA synthesis was performed using a ReverTra Ace™ qPCR RT Master Mix with gRNA Remover (TOYOBO, Japan). The qPCR was conducted using a LightCycle PCR System (Roche Molecular Biochemicals, USA) and SYBR Green Realtime PCR Master Mix (TOYOBO, Japan). Three parallel tests were performed on each sample. Actin was used as the reference gene, and the data were analyzed based on the $2^{-\Delta\Delta CT}$ method [33].

3. Results

3.1. Construction of an alternative NADPH regeneration pathway in a xylose utilization S. cerevisiae

Glucose and xylose compete for the total flux in the non-oxidative

PPP. To prevent glucose from entering the PPP and improve the competitiveness of xylose, as well as decrease the loss of CO_2, the *ZWF1* gene encoding the glucose-6-phosphate dehydrogenase (G6PDH), catalyzing the first step (glucose-6-phosphate to 6-phosphogluconolactone) of the PPP, was knocked out in the xylose utilizing recombinant strain BSGX001 [19]. The resulting strain was named BZ (Table 1). Batch fermentation containing 20 g L^{-1} glucose or 20 g L^{-1} xylose as a carbon source indicated that BZ grew weakly (Fig. 2). Since the non-oxidative genes of the PPP were overexpressed in BZ, it was anticipated that the BZ should smoothly metabolize xylose through the non-oxidative section of PPP. As a result, the intermediate metabolites within the non-oxidative PPP could be obtained by xylose metabolism. Therefore, the weak growth of BZ on xylose suggests that the oxidative PPP is essential for BZ's growth on xylose. Our perspective is that NADPH is more likely to be a limiting factor than 6PGL and 6 PG (Fig. 1).

To generate sufficient NADPH for cell growth in the *zwf1Δ* strain, three heterologous $NADP^+$-dependent glyceraldehyde-3-phosphate dehydrogenase (GAPDH) genes were expressed in the BZ strain instead of the endogenous NAD^+-dependent GAPDH gene *TDH3*, respectively. Specifically, *GDH* (NW_018932882.1) of *Spinacia oleracea* [25], *gapB* (NC_000964.3) of *Bacillus subtilis* [26], and *GDP1* (NC_006042.1) of *Kluyveromyces lactis* [27] were used, and the resulting strains were named BZH, BZB, and BZP1, respectively (Table 1). The results (Fig. 3, Table 2, Fig. S1) of batch fermentations using 20 g L^{-1} glucose and/or 20 g L^{-1} xylose as a carbon source showed that the expression of all the $NADP^+$-dependent GAPDHs restored cell growth to varying extents. In the glucose-xylose co-fermentation, maximum specific growth rates (μ_{max}) of BZH, BZB, and BZP1 were 0.062 ± 0.001 h^{-1}, 0.142 ± 0.002 h^{-1}, and 0.167 ± 0.002 h^{-1}, respectively, 36.5%, 73.6%, and 86.5% of BSGX001, respectively. However, the μ_{max} of BZ was only 0.026 ± 0.001 h^{-1}, which was 13.5% of BSGX001. Consistent with growth, the expression of $NADP^+$-dependent GAPDHs rescued glucose utilization, and the glucose consumption rates ($r_{glucose}$) of BZ, BZH, BZB, and BZP1 were 16.7%, 23.8%, 45.2%, and 82.1% compared to BSGX001, respectively (Table 2). Considering the insufficient NADPH production in the BZ strain and the fact that these GAPDH-catalyzed reactions are linked to NADPH production, Gdp1 is the optimal choice to supply NADPH in the *zwf1Δ* strain among the three $NADP^+$-dependent GAPDH we have tested.

Xylose metabolism of strains was analyzed across different stages of glucose-xylose co-fermentation. First, in the glucose and xylose co-utilizing stage, the xylose consumption rates ($r1_{xylose}$, Table 2) of BZ, BZH, and BZB were lower than BSGX001, while the $r1_{xylose}$ of BZP1 and BSGX001 were similar. This demonstrated that the lower cell biomass caused by *ZWF1* deletion negatively affected xylose utilization in the initial stage. However, the specific xylose consumption rate (consumption rate per gram of dry cell weight) of BZP1 was 0.19 ± 0.01 g g^{-1} DCW h^{-1}, which is 1.2-fold higher than BSGX001 (0.16 ± 0.01 g g^{-1} DCW h^{-1}), during this phase. This indicated that the deletion of *ZWF1*, thereby dedicating the flux of the PPP exclusively to xylose instead of sharing it with glucose, relieved competitive effects of glucose to xylose as expected. Furthermore, in the xylose utilizing stage (after glucose depletion), the xylose consumption rates ($r2_{xylose}$, Table 2) of BZB and BZP1 were 0.22 ± 0.02 g L^{-1} h^{-1} and 0.24 ± 0.01 g L^{-1} h^{-1}, respectively, which are 1.5- and 1.6-fold higher than BSGX001 (0.15 ± 0.00 g L^{-1} h^{-1}). Moreover, BZB and BZP1 showed higher average ethanol production rates and ethanol yields compared to the initial strain BSGX001 (Fig. 3, Table 2). This may be because, in BZB and BZP1, all the fructose-6-phosphate can be metabolized through the EMP instead of partly converting to glucose-6-phosphate and then metabolized through the PPP. This reduced the wasteful metabolic cycling and limited CO_2 release, thus increasing the ethanol production rate and yield.

3.2. Levels of NADPH cofactors in recombinant S. cerevisiae strains

To uncover the relationship between the available NADPH and the xylose utilization capacity, the ratio of [NADPH] and [$NADP^+$] in BSGX001, BZ, and BZP1 strains was characterized. Cell samples were obtained from the cultures after 16 h and 36 h. For BSGX001 and BZP1, the 16-h samples isolated cells in the mid-log phase (glucose-existing phase), and the 36-h samples isolated cells in the xylose-utilizing phase when glucose had been depleted. For BZ, both the 16- and 36-h samples represented slow-growing cells that predominantly utilized glucose (Fig. 3). The results (Fig. 4) showed that at 16 h, within the glucose-existing phase, the [NADPH]/[$NADP^+$] ratio of BZ was notably lower than BSGX001, while the [NADPH]/[$NADP^+$] ratio of BZP1 was only slightly lower compared to BSGX001. This suggested that the removal of *ZWF1* led to an intracellular NADPH shortage, which limited cell growth. The expression of *GDP1* increased the level of NADPH and therefore, supported a high growth rate.

The [NADPH]/[$NADP^+$] ratio of BSGX001 in the xylose-utilizing phase was similar to the glucose-existing phase (Fig. 4). However, the cell quantity (OD_{600}) did not increase during the xylose-utilizing phase (Fig. 3A). These findings indicated that other issues limited cellular growth, so the NADPH generated only needed to meet the requirements to maintain fundamental metabolism for BSGX001. For BZP1, the [NADPH]/[$NADP^+$] ratio in the xylose-utilizing phase was notably lower than in the glucose-existing phase, which may be due to the consumption rate of xylose being lower than the consumption rate of glucose. Therefore, the EMP flux in the xylose-utilizing phase was lower than in the glucose-utilizing phase, and less NADPH was generated via the $NADP^+$-dependent glyceraldehyde-3-phosphate dehydrogenase-catalyzed reaction. Furthermore, the results also demonstrated that the [NADPH]/[$NADP^+$] ratio in BZ after 36 h was significantly higher than in other strains. At that time, only a small amount of glucose was consumed, and the amount of xylose consumed was even lower. We

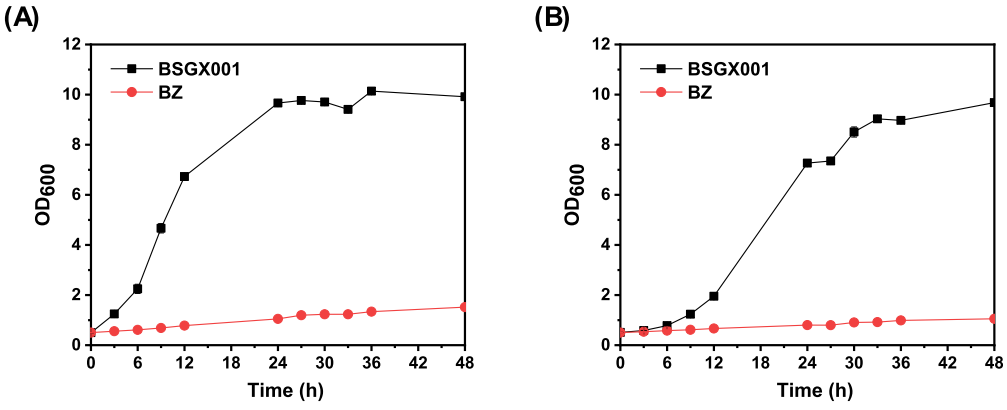

Fig. 2. The growth characteristic of BSGX001 and BZ strains in glucose (A) and xylose (B) fermentation under oxygen-limited condition.

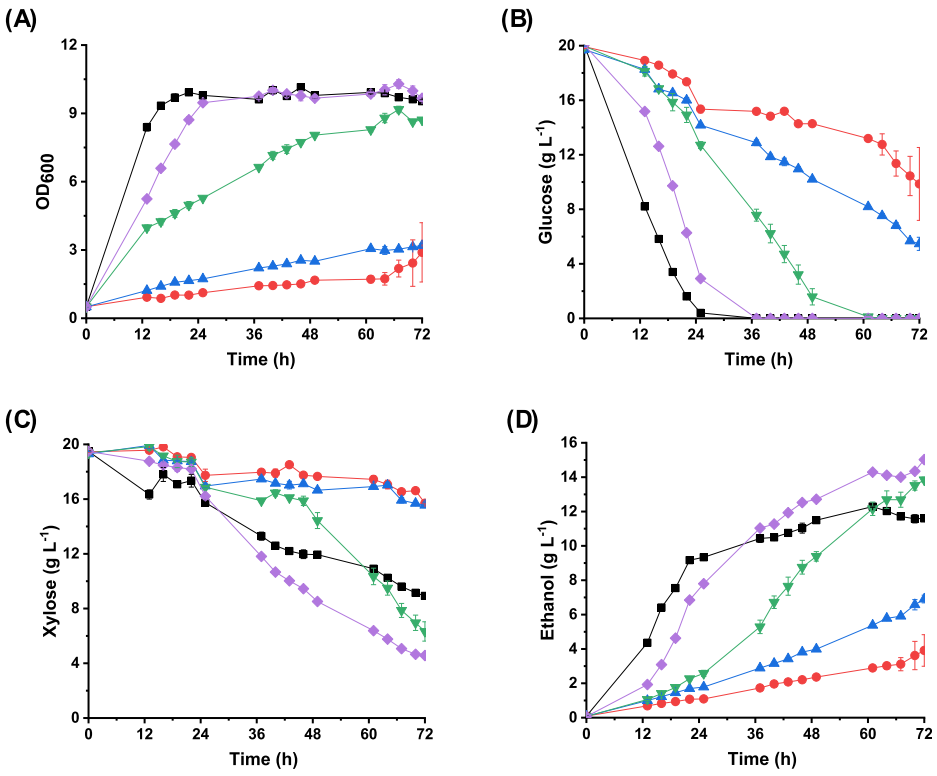

Fig. 3. The co-fermentation characteristics of recombinant strains BSGX001 (■), BZ (●), BZH (▲), BZB (▼), BZP1 (◆). The growth curves (A), glucose consumption (B), xylose consumption (C) and ethanol production (D) of the strains in YNB medium with 20 g L^{-1} glucose and 20 g L^{-1} xylose. Data represent means ± standard deviation of biological triplicates.

Table 2
The fermentation characteristics of recombinant strains.

Strains	μ_{max}[a] (h^{-1})	$r_{glucose}$[a] (g L^{-1} h^{-1})	$r1_{xylose}$[a] (g L^{-1} h^{-1})	$r2_{xylose}$[b] (g L^{-1} h^{-1})	$r_{ethanol}$[c] (g L^{-1} h^{-1})	$Y_{ethanol}$[d] (g g^{-1})
BSGX001	0.193 ± 0.000	0.84 ± 0.01	0.15 ± 0.01	0.15 ± 0.00	0.16 ± 0.00	0.379 ± 0.001
BZ	0.026 ± 0.001	0.14 ± 0.04	0.09 ± 0.02	–	0.05 ± 0.01	0.169 ± 0.034
BZH	0.062 ± 0.001	0.20 ± 0.01	0.08 ± 0.02	–	0.09 ± 0.00	0.292 ± 0.011
BZB	0.142 ± 0.002	0.38 ± 0.01	0.10 ± 0.01	0.22 ± 0.02	0.19 ± 0.00	0.419 ± 0.003
BZP1	0.167 ± 0.002	0.69 ± 0.01	0.14 ± 0.02	0.24 ± 0.01	0.21 ± 0.00	0.430 ± 0.002
BP1R1 (8 h)	0.170 ± 0.004	0.77 ± 0.01	0.09 ± 0.01	0.19 ± 0.00	0.18 ± 0.00	0.428 ± 0.004
BP1R1 (12 h)	0.179 ± 0.000	0.81 ± 0.01	0.14 ± 0.01	0.14 ± 0.00	0.17 ± 0.00	0.423 ± 0.007

[a] The glucose-xylose co-utilization stage.
[b] The glucose depletion and xylose utilization stage.
[c] The stage of whole fermentation.
[d] Ethanol yield of consumed sugars.

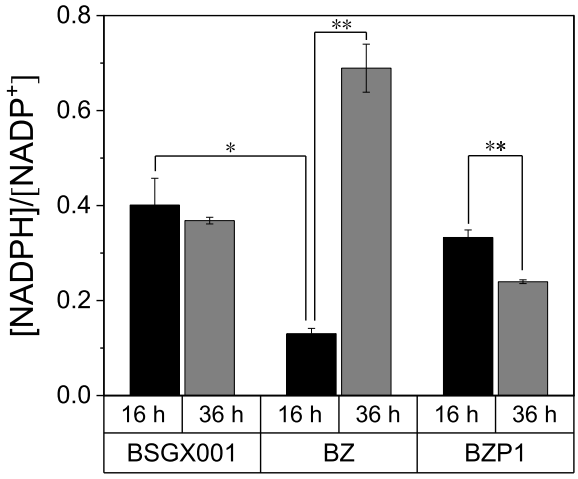

Fig. 4. The [NADPH]/[$NADP^+$] ratio of BSGX001, BZ and BZP1 strains. Samples were taken at 16 h (black columns) and 36 h (gray columns) in glucose-xylose co-fermentation. Experiments were performed in triplicate and the error bars denoted standard deviation from the means of independent experiments.

suspected that the deletion of *ZWF1* decreased the NADPH from PPP. Furthermore, this deletion notably decreased precursors for the synthesis of nucleic acids and amino acids, such as ribose-5-phosphate and erythrose-4-phosphate. This severely hampered cell growth and metabolism. The low growth and metabolism, accompanied by low NADPH consumption, led to the continuous accumulation of NADPH generated from other reactions, such as the glyoxylate cycle, which could turn on when EMP was almost turned off [34].

3.3. Controlling the expression timing of ZWF1 allowed for rapid growth in the early stage and low waste throughout fermentation

To avoid a reduction in cell growth caused by the deletion of *ZWF1* and retain the benefit of NADP $^+$ -dependent GAPDH on xylose utilization, we tried to express *ZWF1* in the early stage of fermentation and turn it off in the following stage in the *GDP1* expressing strain. The *TDH3* of BSGX001 was replaced with *GDP1* resulting in strain BP1, then the promoter of *ZWF1* in BP1 was replaced with P_{CTR1}, inhibited by Cu^{2+} [28,35], resulting in strain BP1R1. The RT-qPCR results uncovered that the expression level of *ZWF1* in BP1R1 was approximately 20% of that in BSGX001 under Cu^{2+} free condition, and the addition of $CuSO_4$ nearly blocked the expression of *ZWF1* (Fig. 5). The glucose-xylose co-fermentation of BP1, BZP1, and BP1R1 was performed at Cu^{2+} free condition. The xylose consumption rate of strains in the following order: BZP1>BP1R1>BP1, indicated that reducing the expression level of *ZWF1* is beneficial for xylose metabolism (Fig. S2).

Glucose-xylose co-fermentation was performed, and 300 μM $CuSO_4$ was added into the fermentation broth of BP1R1 at 8 h and 12 h. The results (Fig. 6, Table 2) demonstrated that the maximum specific growth rates (μ_{max}) of BP1R1 with $CuSO_4$ at 8 h and 12 h were 0.170 ± 0.004 h^{-1} and 0.179 ± 0.000 h^{-1}, respectively, both higher than BZP1 (0.167 ± 0.002 h^{-1}). The glucose consumption rate ($r_{glucose}$) of BP1R1 with $CuSO_4$ at 12 h was 0.81 ± 0.01 g L^{-1} h^{-1}, which was superior to the addition of $CuSO_4$ at 8 h (0.77 ± 0.01 g L^{-1} h^{-1}) and BZP1 (0.69 ± 0.01 g L^{-1} h^{-1}) (Table 2). Furthermore, after glucose depletion, the xylose consumption rate ($r2_{xylose}$) and ethanol production rate ($r_{ethanol}$) of BP1R1 with $CuSO_4$ added at 8 h were higher than adding $CuSO_4$ at 12 h but lower than BZP1 (Table 2). The final ethanol yield ($Y_{ethanol}$) of BP1R1 with $CuSO_4$ at 8 h or 12 h was slightly less than BZP1 (Table 2). These findings indicated that knocking out *ZWF1* is a simple and effective approach to promote xylose metabolism and ethanol production. In the phased control strategy, Zwf1p, which was already expressed before adding $CuSO_4$, might have an ongoing effect, reducing the positive effect of this strategy on ethanol production.

4. Discussion

The xylose utilization efficiency of *S. cerevisiae* severely impacts the economic efficiency of lignocellulosic ethanol production. In glucose-xylose co-fermentation, recombinant *S. cerevisiae* strains typically use glucose more rapidly than xylose. As a result, the glucose is exhausted first, followed by a long-term xylose-utilizing phase. In this work, we blocked the oxidative PPP to prevent the glucose from entering the PPP. This therefore decreasing the competitive inhibition of glucose to xylose utilization. Additionally, we rebuilt an NADPH generation reaction by expressing the NADP$^+$-dependent GAPDH gene in a recombinant *S. cerevisiae* strain with the XI pathway. These operations enhanced the xylose utilization and elevated the ethanol yield, while reducing the glucose metabolism rate. Although we attempted to use novel genes, the *K. lactis* GAPDH gene *GDP1* remained the optimal choice, as previously reported [27]. To account for the decrease in glucose utilization, we further optimized the timing to turn off *ZWF1* expression. The Cu^{2+} repressive promoter *CTR1p* was used to attenuate the expression of *ZWF1*. *ZWF1* expression was turned off after 8 h or 12 h in fermentation by adding Cu^{2+} to the fermentation broth. The results indicated that adding $CuSO_4$ at 8 h and 12 h could promote glucose metabolism. The xylose metabolism and ethanol yield after adding $CuSO_4$ at 8 h were superior to that after adding $CuSO_4$ at 12 h. However, deleting *ZWF1* remains the optimal strategy for high ethanol yield.

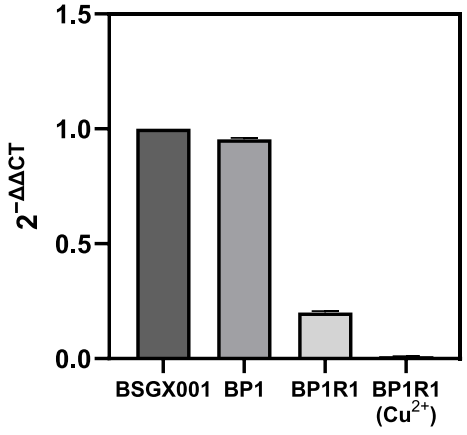

Fig. 5. The transcription level of *ZWF1* in BSGX001, BP1 and BP1R1 (with or without $CuSO_4$).

It is generally believed that glucose inhibits xylose use. The common approach involves enhancing the xylose utilization capacity to boost its competitiveness in co-fermentation. This includes strategies like increasing XI (xylose isomerase) activity and optimizing xylose transport. Recent research has suggested that there is a competition surrounding the flux of PPP and EMP between glucose and xylose, in contrast to the unilateral inhibition of glucose on xylose utilization. Since glucose-xylose co-consumption in high-performance xylose-consuming strains causes the glycolytic flux to be saturated, the excess glucose is phosphorylated and enters the trehalose pathway [36]. Furthermore, an increasing body of evidence indicates that yeast cells enter a state of starvation upon glucose depletion [37]. The expression level of enzymes in the PPP and EMP significantly decreased upon glucose depletion [38]. This is at least in part due to the nutrient-sensing system of yeast not being able to respond to xylose as well as glucose [39,40]. Therefore, an improved strategy would be to moderately reduce glucose consumption in strains with high xylose-utilizing capacity instead of only improving the xylose metabolic capacity. Since reduced glucose metabolism leaves more flux for xylose and prolongs the glucose presence period, it allows cells to keep high PPP and EMP activity because of glucose signal, thus improving overall sugar utilization.

A good example is that reducing glucose metabolism by deleting *HXK2* improved glucose-xylose co-utilization [23]. In contrast, Hxk2p is a bifunctional protein, acting as a transcription factor involved in stress resistance and chronological lifespan, as well as a hexokinase. The expression of $HXK2^{S14A}$ that encodes a constitutively nucleus-localized Hxk2p, increased the xylose consumption and ethanol production rates [41]. Our findings verified that blocking the oxidative PPP is also a good strategy for decreasing glucose utilization rate.

In this work, the deletion of *ZWF1* significantly decreased both glucose and xylose utilization while rebuilding an NADPH generation reaction by expressing NADP $^+$ -dependent glyceraldehyde-3-phosphate dehydrogenase gene partially recovered cell growth (Fig. S1). These results supported the idea that NADPH is crucial for cellular growth and that the shortage of NADPH prevents cells from multiplying. The oxidative PPP is the primary source of NADPH not only in glucose fermentation but also in xylose fermentation in *S. cerevisiae*, as often hypothesized [42,43]. Similar work has been done previously in a recombinant *S. cerevisiae* with the XR-XDH pathway to prevent excess CO_2 releasing and relieve redox imbalance. The deletion of *ZWF1* and expression of NADP $^+$ -dependent GAPDH promoted ethanol production and reduced xylitol production [27]. The cofactor problem in xylose-utilizing *S. cerevisiae* strains with the XI pathway is rarely addressed since the reaction catalyzed by XI does not relate to cofactors like the XR-XDH pathway. However, NADPH is the main reducing agent required for general biosynthesis [24], xylose-utilizing strains with XI also require it for growth. From known metabolic pathways, when glucose is the carbon source, G6P is produced directly by glucose phosphorylation, and approximately 10–15% of G6P enters oxidative PPP [21] to generate NADPH. However, when xylose is the carbon source, the situation becomes complicated. Xylose is phosphorylated to

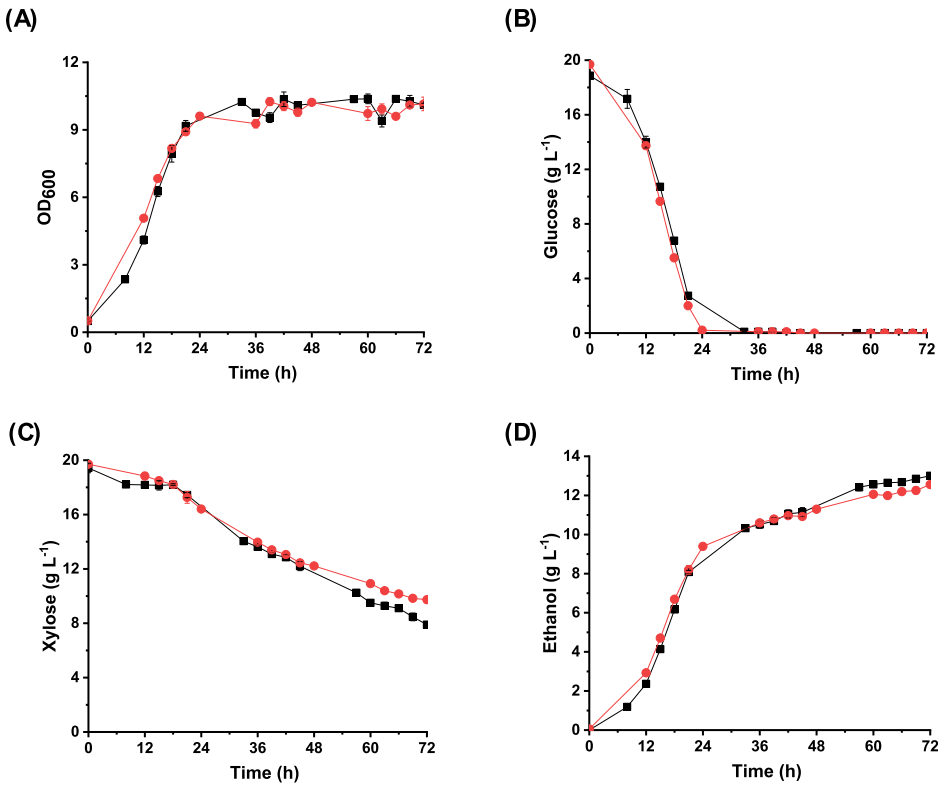

Fig. 6. The co-fermentation characteristics of recombinant strain BP1R1 with adding $CuSO_4$ at 8 h (■) and 12 h (●). The growth curves (A), glucose consumption (B), xylose consumption (C) and ethanol production (D) of the strain in YNB medium with 20 g L^{-1} glucose and 20 g L^{-1} xylose. Data represent means ± standard deviation of biological triplicates.

xylulose 5-phosphate and enters the non-oxidative PPP. Then, glyceraldehyde 3-phosphate (G3P) and fructose 6-phosphate (F6P) are generated through a series of transketone and transaldehyde reactions in the non-oxidative PPP. F6P is then transformed to G6P by phosphoglucose isomerase (PGI), which prefers to catalyze the reaction in the opposite direction [44]. Finally, G6P is further metabolized via the PPP, and cells acquire NADPH (Fig. 1). This process is inefficient and involves a wasteful metabolic cycle. Moreover, the excess carbon dioxide released from the reaction is catalyzed by 6-phosphogluconate dehydrogenase. Our results confirmed that using $NADP^+$-dependent GAPDH reactions instead of the oxidative PPP to generate NADPH significantly increased the xylose consumption rate during the stage at which only xylose remained. Furthermore, the ethanol yield for total consumed sugars increased by 13.5%.

5. Conclusion

Efficient glucose-xylose co-utilization is a critical strategy to fully consume lignocellulosic biomass feedstocks for bioethanol production. In this study, we confirmed that the oxidative PPP is the primary source of NADPH in xylose fermentation, and reconstructed the NADPH regeneration pathway in *S. cerevisiae* by removal of the glucose 6-phosphate dehydrogenase gene *ZWF1* and the replacement of an NAD^+-dependent glyceraldehyde-3-phosphate dehydrogenase gene with an $NADP^+$-dependent one. This operation not only limits the competition of glucose with xylose for pentose phosphate pathway metabolic flux and avoids carbon loss due to excess CO_2 release but also prevents yeast from performing ineffective metabolic cycles to obtain NADPH during the xylose utilization phase. Our work increased the glucose-xylose co-fermentation capacity of yeast and provided new insights into the relationship between NADPH supplying and xylose metabolism in *S. cerevisiae* with the XI pathway.

CRediT authorship contribution statement

Yali Qiu: Conceptualization, Investigation, Methodology, Visualization, Formal analysis, Writing – original draft. **Wei Liu:** Investigation, Writing – review & editing. **Meiling Wu:** Investigation, Formal analysis. **Haodong Bao:** Software, Validation. **Xinhua Sun:** Writing – review & editing. **Qin Dou:** Visualization, Writing – review & editing. **Hongying Jia:** Investigation. **Weifeng Liu:** Supervision, Resources. **Yu Shen:** Conceptualization, Supervision, Funding acquisition, Resources, Writing – review & editing.

Declaration of competing interest

The authors declare that they have no known competing financial interests or personal relationships that could have appeared to influence the work reported in this paper.

Acknowledgements

This work was supported by the National Key Research and Development Program of China (2021YFC2101303), the National Natural Science Foundation of China (32170039).

Appendix A. Supplementary data

Supplementary data to this article can be found online at https://doi.org/10.1016/j.synbio.2024.02.004.

References

[1] Cunha JT, Soares PO, Baptista SL, Costa CE, Domingues L. Engineered *Saccharomyces cerevisiae* for lignocellulosic valorization: a review and perspectives on bioethanol production. Bioengineered 2020;11(1):883–903.

[2] Liu G, Qu Y. Integrated engineering of enzymes and microorganisms for improving the efficiency of industrial lignocellulose deconstruction. Engineering Microbiology 2021;1:100005.
[3] van Maris AJ, Abbott DA, Bellissimi E, van den Brink J, Kuyper M, Luttik MA, Wisselink HW, Scheffers WA, van Dijken JP, Pronk JT. Alcoholic fermentation of carbon sources in biomass hydrolysates by *Saccharomyces cerevisiae*: current status. Antonie Leeuwenhoek 2006;90(4):391–418.
[4] Moysés DN, Reis VC, de Almeida JR, de Moraes LM, Torres FA. Xylose fermentation by *Saccharomyces cerevisiae*: challenges and prospects. Int J Mol Sci 2016;17(3):207.
[5] Shen Y, Chen X, Peng B, Chen L, Hou J, Bao X. An efficient xylose-fermenting recombinant *Saccharomyces cerevisiae* strain obtained through adaptive evolution and its global transcription profile. Appl Microbiol Biotechnol 2012;96(4):1079–91.
[6] van Aalst ACA, de Valk SC, van Gulik WM, Jansen MLA, Pronk JT, Mans R. Pathway engineering strategies for improved product yield in yeast-based industrial ethanol production. Synthetic and systems biotechnology 2022;7(1):554–66.
[7] Hou J, Qiu C, Shen Y, Li H, Bao X. Engineering of *Saccharomyces cerevisiae* for the efficient co-utilization of glucose and xylose. FEMS Yeast Res 2017;17(4).
[8] Xiao C, Pan Y, Huang M. Advances in the dynamic control of metabolic pathways in *Saccharomyces cerevisiae*. Engineering Microbiology 2023;3(4):100103.
[9] Yang S, Song L, Wang J, Zhao J, Tang H, Bao X. Engineering *Saccharomyces cerevisiae* for efficient production of recombinant proteins. Engineering Microbiology 2023:100122.
[10] Jeffries TW, Jin YS. Metabolic engineering for improved fermentation of pentoses by yeasts. Appl Microbiol Biotechnol 2004;63(5):495–509.
[11] Subtil T, Boles E. Competition between pentoses and glucose during uptake and catabolism in recombinant *Saccharomyces cerevisiae*. Biotechnol Biofuels 2012;5:14.
[12] Zhou H, Cheng JS, Wang BL, Fink GR, Stephanopoulos G. Xylose isomerase overexpression along with engineering of the pentose phosphate pathway and evolutionary engineering enable rapid xylose utilization and ethanol production by *Saccharomyces cerevisiae*. Metab Eng 2012;14(6):611–22.
[13] Bergdahl B, Heer D, Sauer U, Hahn-Hägerdal B, van Niel EW. Dynamic metabolomics differentiates between carbon and energy starvation in recombinant *Saccharomyces cerevisiae* fermenting xylose. Biotechnol Biofuels 2012;5(1):34.
[14] Bettiga M, Hahn-Hägerdal B, Gorwa-Grauslund MF. Comparing the xylose reductase/xylitol dehydrogenase and xylose isomerase pathways in arabinose and xylose fermenting *Saccharomyces cerevisiae* strains. Biotechnol Biofuels 2008;1(1):16.
[15] Kuyper M, Hartog MM, Toirkens MJ, Almering MJ, Winkler AA, van Dijken JP, Pronk JT. Metabolic engineering of a xylose-isomerase-expressing *Saccharomyces cerevisiae* strain for rapid anaerobic xylose fermentation. FEMS Yeast Res 2005;5(4–5):399–409.
[16] Endalur Gopinarayanan V, Nair NU. Pentose metabolism in *Saccharomyces cerevisiae*: the need to engineer global regulatory systems. Biotechnol J 2019;14(1):e1800364.
[17] Qi X, Zha J, Liu GG, Zhang W, Li BZ, Yuan YJ. Heterologous xylose isomerase pathway and evolutionary engineering improve xylose utilization in *Saccharomyces cerevisiae*. Front Microbiol 2015;6:1165.
[18] Papapetridis I, Verhoeven MD, Wiersma SJ, Goudriaan M, van Maris AJA, Pronk JT. Laboratory evolution for forced glucose-xylose co-consumption enables identification of mutations that improve mixed-sugar fermentation by xylose-fermenting *Saccharomyces cerevisiae*. FEMS Yeast Res 2018;18(6).
[19] Wei S, Liu Y, Wu M, Ma T, Bai X, Hou J, Shen Y, Bao X. Disruption of the transcription factors Thi2p and Nrm1p alleviates the post-glucose effect on xylose utilization in *Saccharomyces cerevisiae*. Biotechnol Biofuels 2018;11:112.
[20] Wei S, Bai P, Liu Y, Yang M, Ma J, Hou J, Liu W, Bao X, Shen Y. A Thi2p regulatory network controls the post-glucose effect of xylose utilization in *Saccharomyces cerevisiae*. Front Microbiol 2019;10:1649.
[21] Suarez-Mendez CA, Ras C, Wahl SA. Metabolic adjustment upon repetitive substrate perturbations using dynamic (13)C-tracing in yeast. Microb Cell Factories 2017;16(1):161.
[22] Lane S, Turner TL, Jin YS. Glucose assimilation rate determines the partition of flux at pyruvate between lactic acid and ethanol in *Saccharomyces cerevisiae*. Biotechnol J 2023;18(4):e2200535.
[23] Miskovic L, Alff-Tuomala S, Soh KC, Barth D, Salusjärvi L, Pitkänen JP, Ruohonen L, Penttilä M, Hatzimanikatis V. A design-build-test cycle using modeling and experiments reveals interdependencies between upper glycolysis and xylose uptake in recombinant *S. cerevisiae* and improves predictive capabilities of large-scale kinetic models. Biotechnol Biofuels 2017;10:166.
[24] Yukawa T, Bamba T, Guirimand G, Matsuda M, Hasunuma T, Kondo A. Optimization of 1,2,4-butanetriol production from xylose in *Saccharomyces cerevisiae* by metabolic engineering of NADH/NADPH balance. Biotechnol Bioeng 2021;118(1):175–85.
[25] Ferri G, Comerio G, Iadarola P, Zapponi MC, Speranza ML. Subunit structure and activity of glyceraldehyde-3-phosphate dehydrogenase from *spinach chloroplasts*. Biochim Biophys Acta 1978;522(1):19–31.
[26] Kim S, Lee CH, Nam SW, Kim P. Alteration of reducing powers in an isogenic phosphoglucose isomerase (pgi)-disrupted *Escherichia coli* expressing NAD(P)-dependent malic enzymes and NADP-dependent glyceraldehyde 3-phosphate dehydrogenase. Lett Appl Microbiol 2011;52(5):433–40.
[27] Verho R, Londesborough J, Penttilä M, Richard P. Engineering redox cofactor regeneration for improved pentose fermentation in *Saccharomyces cerevisiae*. Appl Environ Microbiol 2003;69(10):5892–7.
[28] Shi H, Jiang Y, Yang Y, Peng Y, Li C. Copper metabolism in *Saccharomyces cerevisiae*: an update. Biometals : an international journal on the role of metal ions in biology, biochemistry, and medicine 2021;34(1):3–14.
[29] Zhang GC, Kong II, Kim H, Liu JJ, Cate JH, Jin YS. Construction of a quadruple auxotrophic mutant of an industrial polyploid *saccharomyces cerevisiae* strain by using RNA-guided Cas9 nuclease. Appl Environ Microbiol 2014;80(24):7694–701.
[30] Jimenez A, Davies J. Expression of a transposable antibiotic resistance element in *Saccharomyces*. Nature 1980;287(5785):869–71.
[31] Li H, Shen Y, Wu M, Hou J, Jiao C, Li Z, Liu X, Bao X. Engineering a wild-type diploid *Saccharomyces cerevisiae* strain for second-generation bioethanol production. Bioresources and bioprocessing 2016;3(1):51.
[32] Peng B, Shen Y, Li X, Chen X, Hou J, Bao X. Improvement of xylose fermentation in respiratory-deficient xylose-fermenting *Saccharomyces cerevisiae*. Metab Eng 2012;14(1):9–18.
[33] Livak KJ, Schmittgen TD. Analysis of relative gene expression data using real-time quantitative PCR and the 2(-Delta Delta C(T)) Method. Methods 2001;25(4):402–8.
[34] Zampar GG, Kümmel A, Ewald J, Jol S, Niebel B, Picotti P, Aebersold R, Sauer U, Zamboni N, Heinemann M. Temporal system-level organization of the switch from glycolytic to gluconeogenic operation in yeast. Mol Syst Biol 2013;9:651.
[35] Xiong X, Chen S. Expanding toolbox for genes expression of *Yarrowia lipolytica* to include novel inducible, repressible, and hybrid promoters. ACS Synth Biol 2020;9(8):2208–13.
[36] Nijland JG, Shin HY, Dore E, Rudinatha D, de Waal PP, Driessen AJM. D-glucose overflow metabolism in an evolutionary engineered high-performance D-xylose consuming *Saccharomyces cerevisiae* strain. FEMS Yeast Res 2021;21(1).
[37] Osiro KO, Brink DP, Borgström C, Wasserstrom L, Carlquist M, Gorwa-Grauslund MF. Assessing the effect of d-xylose on the sugar signaling pathways of *Saccharomyces cerevisiae* in strains engineered for xylose transport and assimilation. FEMS Yeast Res 2018;18(1).
[38] Matsushika A, Nagashima A, Goshima T, Hoshino T. Fermentation of xylose causes inefficient metabolic state due to carbon/energy starvation and reduced glycolytic flux in recombinant industrial *Saccharomyces cerevisiae*. PLoS One 2013;8(7):e69005.
[39] Brink DP, Borgström C, Persson VC, Ofuji Osiro K, Gorwa-Grauslund MF. D-xylose sensing in *Saccharomyces cerevisiae*: insights from D-glucose signaling and native D-xylose utilizers. Int J Mol Sci 2021;22(22).
[40] Qiu Y, Wu M, Bao H, Liu W, Shen Y. Engineering of *Saccharomyces cerevisiae* for co-fermentation of glucose and xylose: current state and perspectives. Engineering Microbiology 2023;3(3):100084.
[41] Zheng L, Wei S, Wu M, Zhu X, Bao X, Hou J, Liu W, Shen Y. Improving xylose fermentation in *Saccharomyces cerevisiae* by expressing nuclear-localized hexokinase 2. Microorganisms 2020;8(6).
[42] Hector RE, Mertens JA, Bowman MJ, Nichols NN, Cotta MA, Hughes SR. *Saccharomyces cerevisiae* engineered for xylose metabolism requires gluconeogenesis and the oxidative branch of the pentose phosphate pathway for aerobic xylose assimilation. Yeast 2011;28(9):645–60.
[43] Sonderegger M, Jeppsson M, Hahn-Hägerdal B, Sauer U. Molecular basis for anaerobic growth of *Saccharomyces cerevisiae* on xylose, investigated by global gene expression and metabolic flux analysis. Appl Environ Microbiol 2004;70(4):2307–17.
[44] Zhang B, Ren L, Zeng S, Zhang S, Xu D, Zeng X, Li F. Functional analysis of PGI1 and ZWF1 in thermotolerant yeast *Kluyveromyces marxianus*. Appl Microbiol Biotechnol 2020;104(18):7991–8006.